

How Well Do Seasonal Climate Anomalies Match Expected El Niño–Southern Oscillation (ENSO) Impacts?

Michelle L. L'Heureux,^a Daniel S. Harnos,^a Emily Becker,^b Brian Brettschneider,^c Mingyue Chen,^a Nathaniel C. Johnson,^d Arun Kumar,^a and Michael K. Tippett^e

KEYWORDS:

North America;
ENSO;
Regression analysis;
Climate variability;
Seasonal variability

ABSTRACT: Did the strong 2023–24 El Niño live up to the hype? While climate prediction is inherently probabilistic, many users compare El Niño events against a deterministic map of expected impacts (e.g., wetter or drier regions). Here, using this event as a guide, we show that no El Niño perfectly matches the ideal image and that observed anomalies will only partially match what was anticipated. In fact, the degree to which the climate anomalies match the expected ENSO impacts tends to scale with the strength of the event. The 2023–24 event generally matched well with ENSO expectations around the United States. However, this will not always be the case, as the analysis shows larger deviations from the historical ENSO pattern of impacts are commonplace, with some climate variables more prone to inconsistencies (e.g., temperature) than others (e.g., precipitation). Users should incorporate this inherent uncertainty in their risk and decision-making analysis.

DOI: 10.1175/BAMS-D-23-0252.1

Corresponding author: Michelle L. L'Heureux, michelle.lheureux@noaa.gov

Manuscript received 25 September 2023, in final form 5 June 2024, accepted 25 June 2024

© 2024 American Meteorological Society. This published article is licensed under the terms of the default AMS reuse license. For information regarding reuse of this content and general copyright information, consult the AMS Copyright Policy (www.ametsoc.org/PUBSReuseLicenses).

AFFILIATION: ^a NOAA/NWS/NCEP/Climate Prediction Center, College Park, Maryland; ^b University of Miami, Cooperative Institute for Marine and Atmospheric Studies, Coral Gables, Florida; ^c NOAA/National Weather Service Alaska Region Headquarters, Anchorage, Alaska; ^d NOAA/OAR/Geophysical Fluid Dynamics Laboratory, Princeton, New Jersey; ^e Department of Applied Physics and Applied Mathematics, Columbia University, New York, New York

1. Introduction

Widespread public interest in the strong El Niño of 2023–24 generated an expectation that weather and climate impacts across the United States would appear similar to a “typical” El Niño. Operational climate forecasters are careful to caveat these expectations by providing probabilities for a range of outcomes (Barnston et al. 2010; Peng et al. 2012), e.g., an increased chance of above-average winter temperatures across the northern United States; yet, these cautions are often brushed aside when users look back at the season to examine what actually happened. They will ask, did 2023–24 resemble the typical impacts from a strong El Niño? Cases that do not conform to one’s prior assumptions are sometimes regarded as a “bust,” or a situation where El Niño’s impacts failed to materialize. Despite careful efforts by meteorological services to convey probabilities, many users ultimately judge the success or failure of an El Niño by how well it resembled the expected impacts.

The strong El Niño of 1997–98 sets the stage for expectations for future events (McPhaden 1999). With a distinctive stripe of wetter-than-average conditions across the southern tier of the United States, drier conditions in the Pacific Northwest and Ohio Valley, warmer temperatures over the northern United States, and cooler temperatures across the South, this winter aligned well with the anticipated impacts from El Niño (Barnston et al. 1999). However, alongside those years that conformed to the canonical impacts of El Niño, there are also some cases which defied expectations, such as the strong 2015–16 El Niño, with drier-than-average conditions occurring in some regions where it had been anticipated to be wetter (Chen and Kumar 2018). Is this latter case an instance when something had gone seriously awry with El Niño? Or was it an example where other factors came into play, which caused the observed impacts to deviate from expectations? To begin unraveling these questions, we seek to provide a baseline to compare historical cases with the expected ENSO impacts. El Niño events rarely resemble 1997–98, so how should we evaluate the quality of the impact, such as what was observed in 2023–24?

Climate researchers seek to distinguish and communicate predictable climate “signals” from unpredictable “noise,” or chaotic weather (Kumar and Hoerling 1995; Doblas-Reyes et al. 2013; Jha et al. 2019). ENSO is considered a leading predictable signal for seasonal climate because preceding anomalies in the ocean form many months in advance of the peak impacts. However, even in its more extreme states, ENSO explains a limited amount of seasonal climate variability over the United States, with deviations from the expectation arising from other possible sources of predictability, or, more often, contribution from noise that cannot be anticipated in advance (Peng et al. 2019; Swenson et al. 2019; Kumar and Chen 2020). There is evidence that different flavors of El Niño can lead to diverse impacts over the United States (Capotondi et al. 2015; Shi et al. 2019), but there is debate whether those differences

are robust or reflect random internal atmospheric variability, which is large over extratropical regions (Kumar and Hoerling 1997; Deser et al. 2017).

Anthropogenic climate change trends likely have an increasing influence on seasonal climate anomalies (Peng et al. 2012). While important, these more slowly evolving forcings are independent of the seasonal mechanisms of ENSO itself. Therefore, to focus on ENSO impacts, data are linearly detrended across the period of record. It is the spread around the expected ENSO pattern of impacts (hereafter, ENSO pattern) that often leads to the most consternation among users, who would prefer to place their bets on a single, fixed El Niño pattern—not the deviations from it. Here, we provide a benchmark for what users should actually expect by comparing observed climatic anomalies against historical ENSO expectations.

2. Evaluating expected ENSO impacts

Here, “expected ENSO impacts” is taken to be the ENSO regression pattern, which is the regression of climate anomalies onto the Niño-3.4 index (Bamston et al. 1997). ERSSTv5 is used to compute the index (Huang et al. 2017). These patterns are the basis for numerous schematics and diagrams that describe the influence of ENSO on climate anomalies (Lindsey 2017). To facilitate comparison with observed anomalies, the regression map is multiplied by the observed Niño-3.4 index values; this is called the “ENSO reconstruction.” The results are not substantively different if we substitute composites for the regression maps. Notably, the ENSO reconstructions are linear and are based on the historical record of ENSO events, which contains uncertainty (Deser et al. 2017, 2018).

We use pattern correlation (with map means removed) to measure the similarity between observed climate anomalies and ENSO regression patterns. Data are cosine weighted by latitude. Pattern correlation coefficients (r_p) vary between -1 and $+1$ with values close to $+1$ indicating strong spatial similarity between the observations and the expected El Niño pattern. Values close to -1 indicate similarity to La Niña. The correlation coefficient provides information on the amount of variability explained. For example, a pattern correlation coefficient of 0.8 means 64% of the observed spatial variability is described by the ENSO pattern ($0.8^2 \times 100 = 64$). Pattern correlations at or near zero indicate that the ENSO pattern had little-to-no relation with the observed anomalies.

We focus mostly on December–February (DJF) 1959–2024, which matches the NOAA winter outlook target period and is a time of year when ENSO impacts are typically strong. January–March and February–April are also suitable candidates and may show even stronger relationships for certain regions and variables (Livezey et al. 1997; Kumar and Hoerling 1998). We also investigate ENSO’s impacts on the Atlantic hurricane season, August–October (ASO 1959–2023), which is a season when ENSO is still developing prior to its wintertime maximum.

3. Circulation anomalies across the Pacific–North America region

Figure 1 shows the DJF 2023–24 average 500-mb (1 mb = 1 hpa) geopotential height anomalies (top left), the “expected” ENSO map or the reconstruction for DJF 2023–24 (bottom left), and a scatterplot of the historical pattern correlations (r_p) for 2023–24 (star) and previous DJF seasons as a function of the Oceanic Niño Index (ONI) value (which is the 3-month average SST anomaly in the Niño-3.4 region). Each dot is accompanied by a two-digit year label corresponding to January–February. A thick black line is a least squares fit (“best fit”) placed where it minimizes the distance between the line and all dots in the vertical. This best fit line provides an estimate of the average pattern correlation that may accompany a given ONI value. In the top-left corner of the diagram is another correlation coefficient (r , which is distinct from the pattern correlations, r_p) that specifies how strongly the ONI varies with

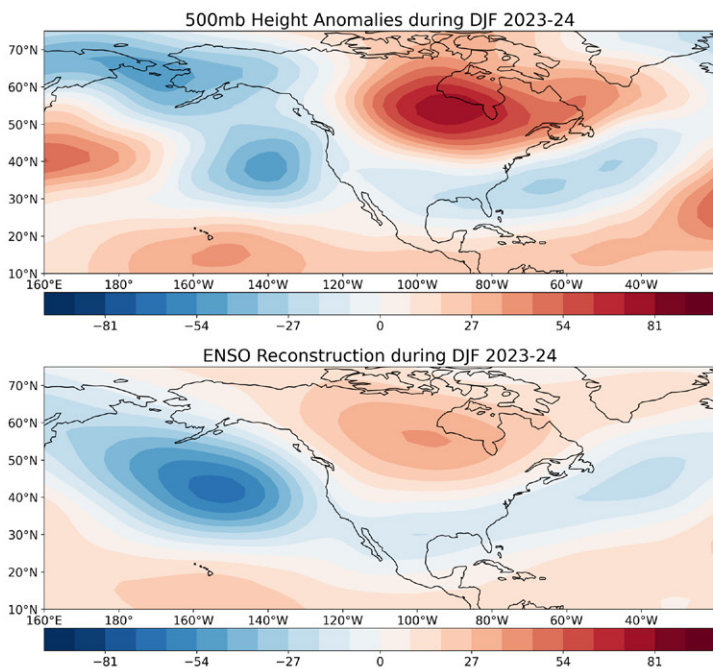


FIG. 1. (top left) Observed DJF 2023–24 average 500-mb geopotential height anomalies (m), (bottom left) the ENSO reconstruction for DJF 2023–24, and a scatterplot of pattern correlations (r_p on y axis) against ONI values (x axis). DJF 2023–24 is shown by the black star. The DJF 2023–24 pattern correlation was ranked fifth most positive in the historical record (92nd percentile). Each dot is accompanied by a two-digit year label corresponding to January–February. A least squares linear regression between the ONI values and pattern correlations is also displayed. Data are based on NCEP/NCAR reanalysis (Kalnay et al. 1996).

the pattern correlations between each winter's anomalies and the expected ENSO pattern. If all the dots were located on the best fit line, then r would be equal to 1.0 and 100% of the variability in the ONI would be explained by the pattern correlation (or vice versa). A coefficient close to 0 would imply a cloud of dots with no clear orientation, so even though some winters may match well with the expected ENSO map, there is no overall relationship with the intensity of ONI.

Figure 1—and subsequent figures—highlights two key features about the relationship between ENSO and climatic variables. First, the best fit line has a positive slope, revealing stronger ONI values, in either the positive (El Niño) or negative (La Niña) direction, are accompanied by larger correlations (better matches) between the DJF winter and the expected ENSO pattern. Second, the pattern correlation displays a certain amount of scatter around the best fit, with only a few years lying nearly on top of the line (in Fig. 1, 1982–83, for example). Observations that lie near or on the best fit line have pattern correlations that could be anticipated based on historical ONI values. Notably, even with the strongest ENSO events, no year will perfectly match the expected ENSO map. Deviations from the expected ENSO pattern can arise from intrinsic variability that accompanies ENSO, or other factors (e.g., noise/weather chaos, Madden–Julian oscillation, Arctic Oscillation, nonlinearity, and other boundary forcings) that cause the observations to deviate from the expected ENSO pattern.

During the strong El Niño of 2023–24, the pattern correlation between the observed height anomalies and the expected ENSO anomalies, as shown by the reconstruction, was quite large ($r_p = 0.68$, Fig. 1). It is a coincidence that the r_p value for 2023–24 equals r displayed in the top-left corner. The centers of action in the Pacific–North American region aligned quite well with the classic El Niño wave train that extends, with alternating height anomalies, from Hawaii to the southeastern United States (Horel and Wallace 1981).

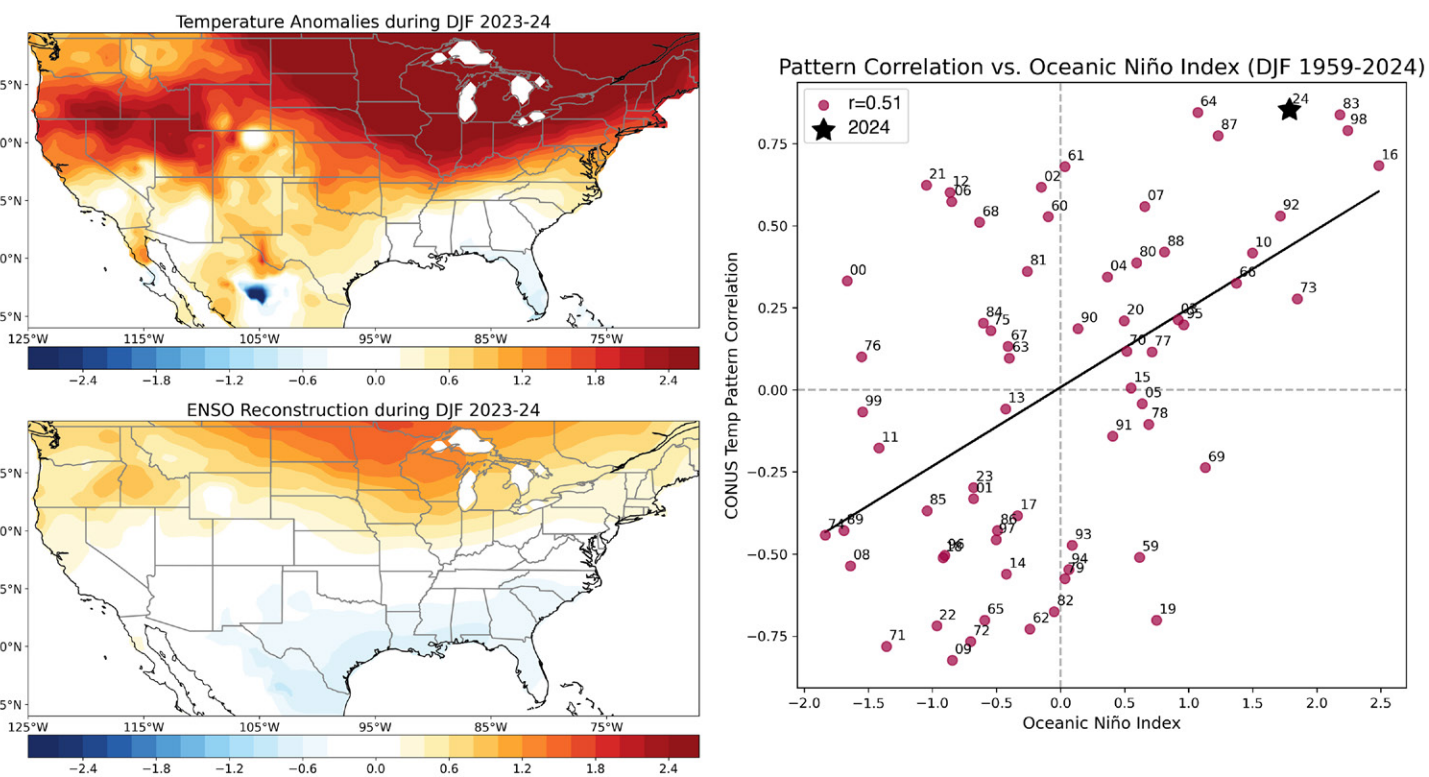


FIG. 2. As in Fig. 1, but displaying 2-m temperature ($^{\circ}$ C) from Global Historical Climatology Network (GHCN)-Climate Anomaly Monitoring System (CAMS) (Fan and van den Dool 2008). The DJF 2023–24 pattern correlation was the most positive in the historical record.

4. Surface temperature anomalies across the contiguous United States

The ONI describes roughly 25% of the variance in the winter-to-winter ENSO pattern correlations for surface air temperature across the contiguous United States (CONUS) ($r = 0.51$, Fig. 2). While the range of pattern correlations for air temperature is roughly the same as the 500-hPa geopotential heights (cf. y axes), it is clear that the spread about the best fit line is larger for temperature. The spread is also not evenly distributed around the best fit line, in the sense that some moderate-to-strong La Niña winters ($\leq -1.0^{\circ}$ C) have had positive pattern correlations (winters that looked more like El Niño), whereas it is quite rare to see a moderate-to-strong El Niño with negative pattern correlations (e.g., 1968–69). While the data are linearly detrended, this asymmetry suggests some nonlinearity with El Niño in the sense that stronger El Niño are accompanied by additional warming not removed by the subtraction of the linear trend.

The observed DJF 2023–24 temperature anomalies had a high pattern correlation with the ENSO reconstruction ($r_p = 0.85$), among the largest historically. However, while above-average temperatures were observed across the northern part of the country, it is clear that the intensity of the positive anomalies was greater in the observations. Moreover, the observed pattern of cooling was not as widespread in the southern United States as in the reconstruction.

5. Precipitation anomalies across the contiguous and southwestern United States

CONUS precipitation anomalies have the strongest relationship between the ONI and the pattern correlations shown herein ($r = 0.78$, Fig. 3). Thus, the strength of ENSO is strongly related to the likelihood of a match between the ENSO pattern and the observed anomalies. For the DJF 2023–24 observed anomalies, the pattern correlation (r_p) with ENSO was 0.39 and was nearly on top of the best fit line, meaning that the pattern correlation fits well with historical expectations for an El Niño of the given strength. Consistent with El Niño, above-average

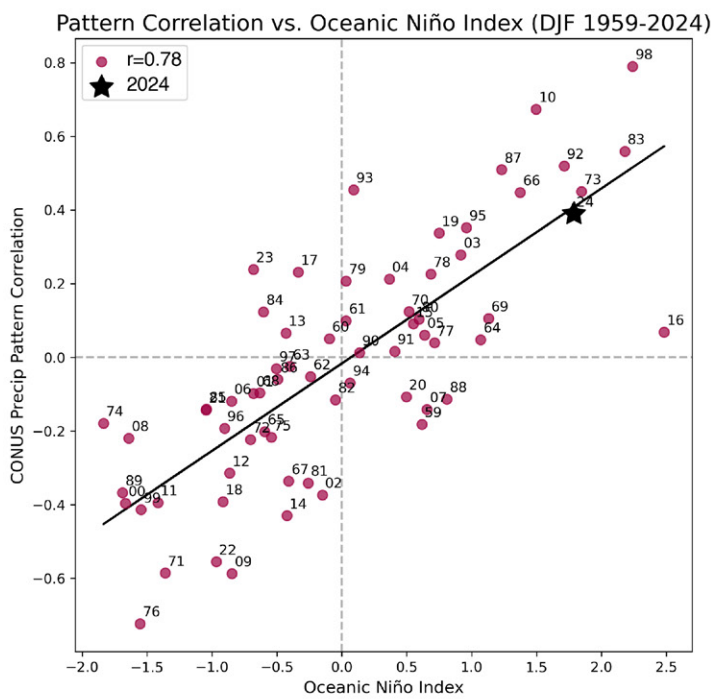
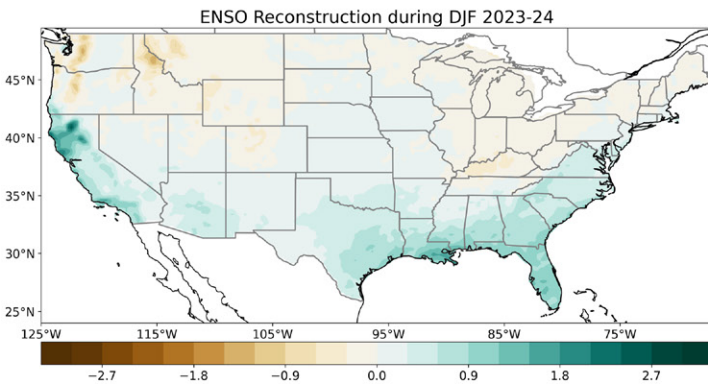
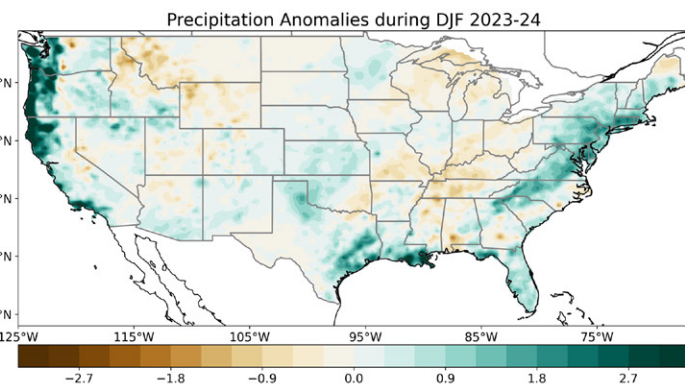


FIG. 3. As in Fig. 1, but displaying precipitation (mm day^{-1}) from CPC unified gauge-based analysis (Chen et al. 2008). The DJF 2023–24 pattern correlation was ranked ninth most positive in the historical record (86th percentile).

precipitation extended across most of the southern CONUS, with drier conditions observed in the Ohio–Tennessee Valley and northern Rockies (L’Heureux et al. 2015; Deser et al. 2018). Similar to CONUS temperature, the strongest amplitude El Niño events tend to lie above the best fit line, hinting at nonlinearity (Hoell et al. 2016). As shown next, precipitation across the southwestern United States shares the same feature.

ENSO describes large-scale anomalies better than those at smaller scales, and the role of internal variability and other factors becomes more significant for regional and local analyses. Focusing on precipitation anomalies around the southwestern United States, stronger ENSO events tilt the odds for a larger match between the observations and expected ENSO pattern, but there are numerous deviations from the best fit line ($r = 0.43$; Fig. 4). In 2023–24, the pattern correlation (r_p) was 0.59, but during the stronger 2015–16 El Niño (L’Heureux et al. 2017), the pattern correlation was substantially lower, though not an outlier given the typical spread for this domain and variable. Relative to the southwest, the southeastern United States has a stronger and more statistically significant relationship between variability in the pattern correlations and ENSO ($r = 0.6$, not shown). However, the pattern correlations are more strongly related to winter-to-winter ONI variability for the entire CONUS domain (Fig. 3) than for either of these smaller regions within the CONUS.

6. Snowfall anomalies across the contiguous United States

Unlike precipitation, DJF 2023–24 snowfall was not characterized by distinctive positive anomalies across the southern half of the CONUS (Fig. 5), implying that anomalous rainfall rather than snowfall generally accompanied the southward shifted storm track. The predominance of rainfall is also consistent with the well above-average temperatures observed during 2023–24 (Fig. 2). However, the northern areas that tend to have snowfall deficits during El Niño were nearly replicated in the DJF 2023–24 observations, which meant the pattern correlation was positive, though not large ($r_p = 0.29$). Over the longer historical record, snowfall

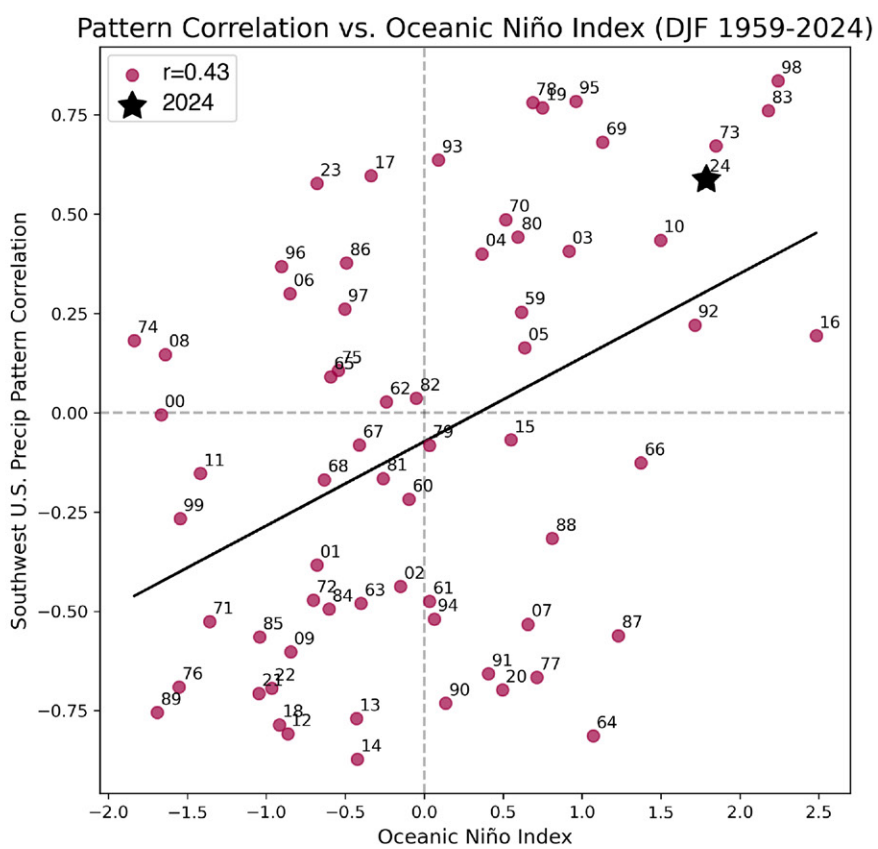
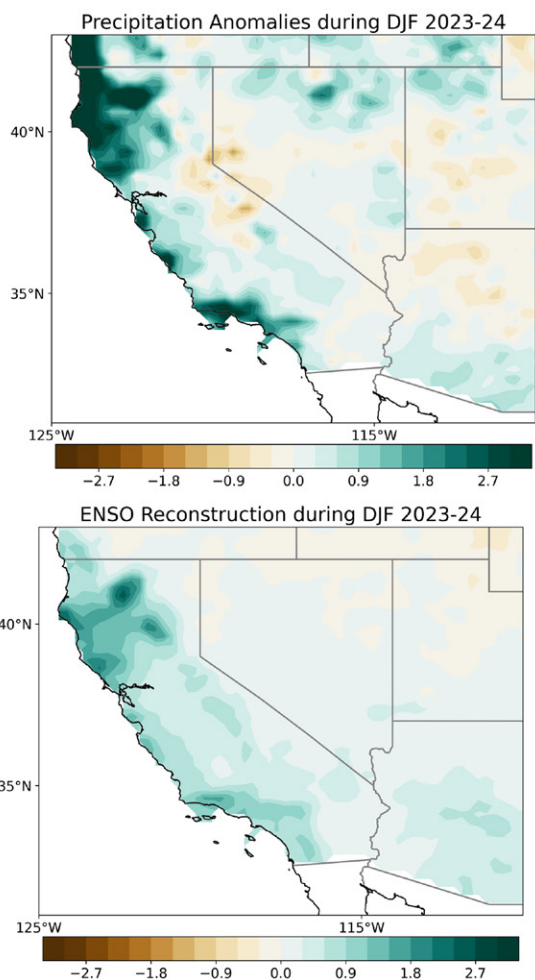


FIG. 4. As in Fig. 3, but focusing on precipitation anomalies (mm day^{-1}) for the southwestern United States. The DJF 2023–24 pattern correlation was ranked 10th most positive in the historical record (85th percentile).

anomaly patterns are not as strongly linked to the ONI ($r = 0.57$, Fig. 5) compared to precipitation anomalies ($r = 0.78$, Fig. 3), which suggests dependence on temperature anomalies which have a lower relation with the ONI ($r = 0.51$).

7. Vertical wind shear anomalies around the tropical Atlantic

El Niño typically corresponds to reduced vertical wind shear over the eastern Pacific and increased wind shear over the Caribbean Sea through central Atlantic (Gray 1984; Bell and Chelliah 2006; Wang et al. 2014). Historically, this relationship has been relatively strong, with ENSO explaining about 49% of the variability in the pattern correlations of ASO wind shear magnitude, here defined as the absolute value of the difference in zonal winds between 200 and 850 mb ($r = 0.7$, Fig. 6). While not the only factor in a hurricane season, vertical wind shear is one key ingredient that can determine whether a hurricane season is active or not. In ASO 2023, many of the features that typically accompany El Niño were absent, as reflected by the near-zero pattern correlation, which is among the lowest for a strong El Niño. Instead, mostly reduced wind shear was evident across the Caribbean and extended into the tropical Atlantic, likely contributing to the above-average hurricane season with 20 named storms, 7 hurricanes, and 3 major hurricanes. Klotzbach et al. (2024) found that the very warm tropical Atlantic partially drove the reduced vertical wind shear compared to other larger El Niño events. Near the Gulf of Mexico and southeastern CONUS, higher wind shear may have helped to reduce landfalling tropical cyclones (NHC 2024).

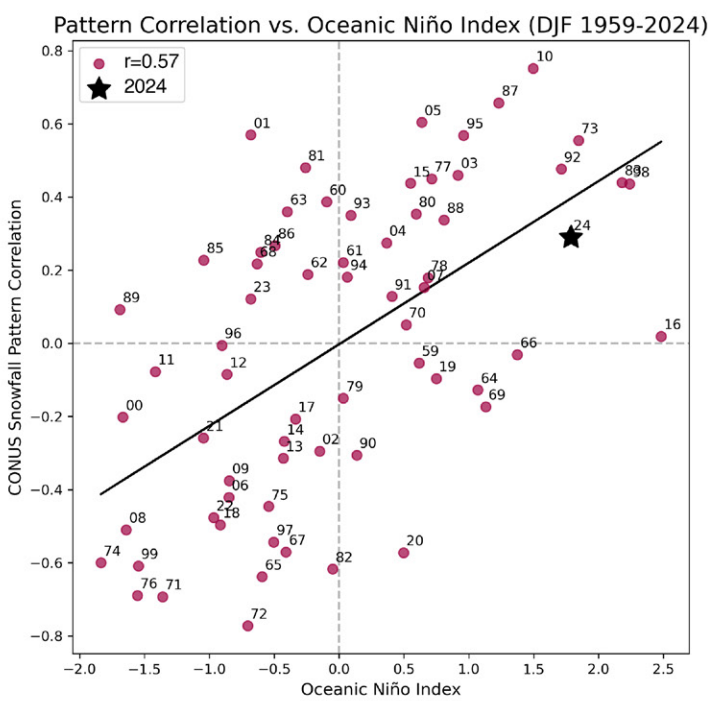
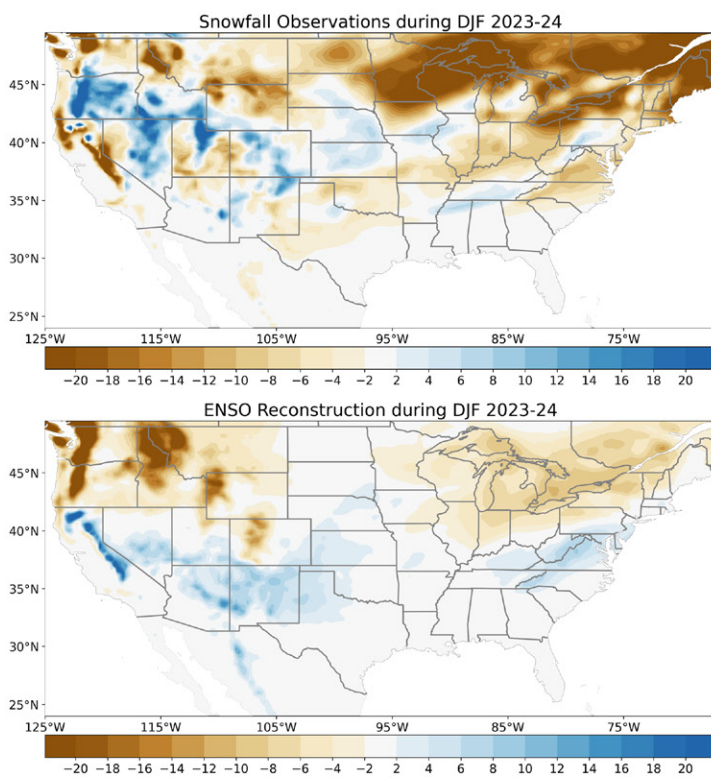


FIG. 5. As in Fig. 1, but displaying snowfall (in.) from the ERA5 reanalysis (Hersbach et al. 2020). The DJF 2023–24 pattern correlation was ranked 19th most positive in the historical record (71st percentile).

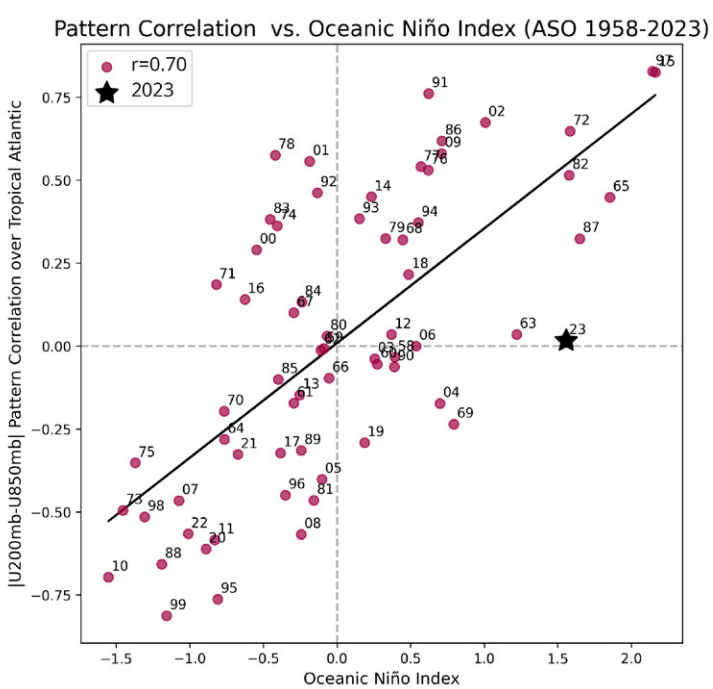
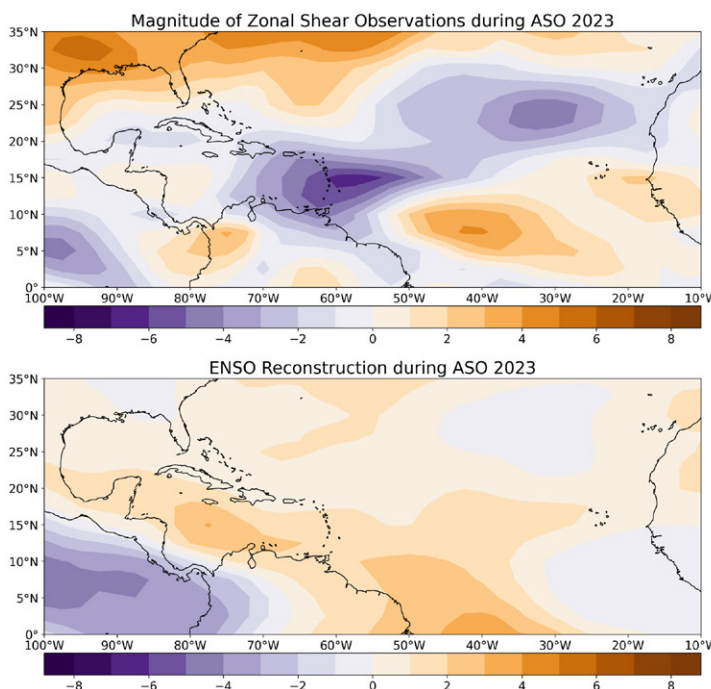


FIG. 6. As in Fig. 1, but focusing on the magnitude of the ASO 200–850-mb zonal wind shear anomalies (m s^{-1}) from NCEP/NCAR reanalysis (Kalnay et al. 1996). The ASO 2023 pattern correlation was ranked 32nd most positive in the historical record (52nd percentile).

8. Key points

We have examined historical relationships between various variables and domains with ENSO, highlighting the strong 2023–24 El Niño. Several key messages emerge from the analysis:

- 1) Observed climate anomalies better resemble the overall ENSO pattern the stronger the ENSO event. Weaker events generally have weaker pattern correlations (r_p) between observations and the expected ENSO impact.
- 2) Any given year can have weaker or stronger matches with the ENSO pattern than expected. Some years can deviate strongly from expectations, as has been the case throughout history and does not imply that the ENSO phenomenon itself went awry.
- 3) The relationship between ENSO's strength and how well the observations match ENSO will depend on the variable and geographic domain. For instance, the correlation (r) is stronger for CONUS precipitation but is not as strong for CONUS temperature or smaller domains, such as southwest precipitation.
- 4) Within a specific season, the resemblance to ENSO can be stronger for certain variables and domains and less so for others. For instance, 2023–24 had a high pattern correlation (r_p) for DJF CONUS temperature and a low pattern correlation for ASO tropical Atlantic wind shear.

While the analysis provided is diagnostic, and not prognostic (which also takes into account climate trends and other seasonal drivers), this perspective helps to provide realistic expectations for climate anomalies during any given ENSO season.

Acknowledgments. We thank Matt Rosencrans, Zeng-Zhen Hu, Mike McPhaden, and three anonymous reviewers for their comments, which helped to improve the manuscript. The scientific results and conclusions, as well as any view or opinions expressed herein, are those of the authors and do not necessarily reflect the views of NWS, NOAA, or the Department of Commerce.

Data availability statement. The ONI was provided by NOAA CPC, from their website at <https://www.cpc.ncep.noaa.gov/data/indices/>. Geopotential height, winds, temperature, and precipitation data were provided by the NOAA Physical Sciences Laboratory, Boulder, Colorado, USA, from their website at <https://psl.noaa.gov>. ERA5 data were retrieved from the Copernicus Climate Data Store, from their website at <https://cds.climate.copernicus.eu/cdsapp>.

References

Bamston, A. G., M. Chelliah, and S. B. Goldenberg, 1997: Documentation of a highly ENSO-related SST region in the equatorial Pacific: Research note. *Atmos.–Ocean*, **35**, 367–383, <https://doi.org/10.1080/07055900.1997.9649597>.

Barnston, A. G., A. Leetmaa, V. E. Kousky, R. E. Livezey, E. A. O’Lenic, H. V. den Dool, A. J. Wagner, and D. A. Unger, 1999: NCEP forecasts of the El Niño of 1997–98 and its U.S. impacts. *Bull. Amer. Meteor. Soc.*, **80**, 1829–1852, [https://doi.org/10.1175/1520-0477\(1999\)080<1829:NFOTEN>2.0.CO;2](https://doi.org/10.1175/1520-0477(1999)080<1829:NFOTEN>2.0.CO;2).

—, S. Li, S. J. Mason, D. G. DeWitt, L. Goddard, and X. Gong, 2010: Verification of the first 11 years of IRI’s seasonal climate forecasts. *J. Appl. Meteor. Climatol.*, **49**, 493–520, <https://doi.org/10.1175/2009JAMC2325.1>.

Bell, G. D., and M. Chelliah, 2006: Leading tropical modes associated with interannual and multidecadal fluctuations in North Atlantic Hurricane activity. *J. Climate*, **19**, 590–612, <https://doi.org/10.1175/JCLI3659.1>.

Capotondi, A., and Coauthors, 2015: Understanding ENSO diversity. *Bull. Amer. Meteor. Soc.*, **96**, 921–938, <https://doi.org/10.1175/BAMS-D-13-00117.1>.

Chen, M., and A. Kumar, 2018: Winter 2015/16 atmospheric and precipitation anomalies over North America: El Niño response and the role of noise. *Mon. Wea. Rev.*, **146**, 909–927, <https://doi.org/10.1175/MWR-D-17-0116.1>.

—, W. Shi, P. Xie, V. B. S. Silva, V. E. Kousky, R. Wayne Higgins, and J. E. Janowiak, 2008: Assessing objective techniques for gauge-based analyses of global daily precipitation. *J. Geophys. Res.*, **113**, D04110, <https://doi.org/10.1029/2007JD009132>.

Deser, C., I. R. Simpson, K. A. McKinnon, and A. S. Phillips, 2017: The Northern Hemisphere extratropical atmospheric circulation response to ENSO: How well do we know it and how do we evaluate models accordingly? *J. Climate*, **30**, 5059–5082, <https://doi.org/10.1175/JCLI-D-16-0844.1>.

—, —, A. S. Phillips, and K. A. McKinnon, 2018: How well do we know ENSO’s climate impacts over North America, and how do we evaluate models accordingly? *J. Climate*, **31**, 4991–5014, <https://doi.org/10.1175/JCLI-D-17-0783.1>.

Doblas-Reyes, F. J., J. Garcia-Serrano, F. Lienert, A. P. Biescas, and L. R. L. Rodrigues, 2013: Seasonal climate predictability and forecasting: Status and prospects. *Wiley Interdiscip. Rev.: Climate Change*, **4**, 245–268, <https://doi.org/10.1002/wcc.217>.

Fan, Y., and H. van den Dool, 2008: A global monthly land surface air temperature analysis for 1948–present. *J. Geophys. Res.*, **113**, D01103, <https://doi.org/10.1029/2007JD008470>.

Gray, W. M., 1984: Atlantic seasonal hurricane frequency. Part I: El Niño and 30 mb quasi-biennial oscillation influences. *Mon. Wea. Rev.*, **112**, 1649–1668, [https://doi.org/10.1175/1520-0493\(1984\)112<1649:ASHFPI>2.0.CO;2](https://doi.org/10.1175/1520-0493(1984)112<1649:ASHFPI>2.0.CO;2).

Hersbach, H., and Coauthors, 2020: The ERA5 global reanalysis. *Quart. J. Roy. Meteor. Soc.*, **146**, 1999–2049, <https://doi.org/10.1002/qj.3803>.

Hoell, A., M. Hoerling, J. Eischeid, K. Wolter, R. Dole, J. Perlitz, T. Xu, and L. Cheng, 2016: Does El Niño intensity matter for California precipitation? *Geophys. Res. Lett.*, **43**, 819–825, <https://doi.org/10.1002/2015GL067102>.

Horel, J. D., and J. M. Wallace, 1981: Planetary-scale atmospheric phenomena associated with the Southern Oscillation. *Mon. Wea. Rev.*, **109**, 813–829, [https://doi.org/10.1175/1520-0493\(1981\)109<0813:PSAPAW>2.0.CO;2](https://doi.org/10.1175/1520-0493(1981)109<0813:PSAPAW>2.0.CO;2).

Huang, B., and Coauthors, 2017: Extended Reconstructed Sea Surface Temperature, version 5 (ERSSTv5): Upgrades, validations, and intercomparisons. *J. Climate*, **30**, 8179–8205, <https://doi.org/10.1175/JCLI-D-16-0836.1>.

Jha, B., A. Kumar, and Z.-Z. Hu, 2019: An update on the estimate of predictability of seasonal mean atmospheric variability using North American Multi-Model Ensemble. *Climate Dyn.*, **53**, 7397–7409, <https://doi.org/10.1007/s00382-016-3217-1>.

Kalnay, E., and Coauthors, 1996: The NCEP/NCAR 40-Year Reanalysis Project. *Bull. Amer. Meteor. Soc.*, **77**, 437–472, [https://doi.org/10.1175/1520-0477\(1996\)077<0437:TNYRP>2.0.CO;2](https://doi.org/10.1175/1520-0477(1996)077<0437:TNYRP>2.0.CO;2).

Klotzbach, P. J., and Coauthors, 2024: The 2023 Atlantic hurricane season: An above-normal season despite strong El Niño conditions. *Bull. Amer. Meteor. Soc.*, <https://doi.org/10.1175/BAMS-D-23-0305.1>, in press.

Kumar, A., and M. P. Hoerling, 1995: Prospects and limitations of seasonal atmospheric GCM predictions. *Bull. Amer. Meteor. Soc.*, **76**, 335–345, [https://doi.org/10.1175/1520-0477\(1995\)076<0335:PALOSA>2.0.CO;2](https://doi.org/10.1175/1520-0477(1995)076<0335:PALOSA>2.0.CO;2).

—, and —, 1997: Interpretation and implications of the observed inter–El Niño variability. *J. Climate*, **10**, 83–91, [https://doi.org/10.1175/1520-0442\(1997\)010<0083:IAIOTD>2.0.CO;2](https://doi.org/10.1175/1520-0442(1997)010<0083:IAIOTD>2.0.CO;2).

—, and —, 1998: Annual cycle of Pacific–North American seasonal predictability associated with different phases of ENSO. *J. Climate*, **11**, 3295–3308, [https://doi.org/10.1175/1520-0442\(1998\)011<3295:ACOPNA>2.0.CO;2](https://doi.org/10.1175/1520-0442(1998)011<3295:ACOPNA>2.0.CO;2).

—, and M. Chen, 2020: Understanding skill of seasonal mean precipitation prediction over California during boreal winter and role of predictability limits. *J. Climate*, **33**, 6141–6163, <https://doi.org/10.1175/JCLI-D-19-0275.1>.

L’Heureux, M. L., M. K. Tippett, and A. G. Barnston, 2015: Characterizing ENSO coupled variability and its impact on North American seasonal precipitation and temperature. *J. Climate*, **28**, 4231–4245, <https://doi.org/10.1175/JCLI-D-14-00508.1>.

—, and Coauthors, 2017: Observing and predicting the 2015/16 El Niño. *Bull. Amer. Meteor. Soc.*, **98**, 1363–1382, <https://doi.org/10.1175/BAMS-D-16-0009.1>.

Lindsey, R., 2017: How El Niño and La Niña affect the winter jet stream and U.S. climate. NOAA Climate.gov, accessed 21 March 2024, <https://www.climate.gov/news-features/featured-images/how-el-nio-and-la-nia-affect-winter-jet-stream-and-us-climate/>.

Livezey, R. E., M. Masutani, A. Leetmaa, H. Rui, M. Ji, and A. Kumar, 1997: Teleconnective response of the Pacific–North American region atmosphere to large central equatorial Pacific SST anomalies. *J. Climate*, **10**, 1787–1820, [https://doi.org/10.1175/1520-0442\(1997\)010<1787:TROTPN>2.0.CO;2](https://doi.org/10.1175/1520-0442(1997)010<1787:TROTPN>2.0.CO;2).

McPhaden, M. J., 1999: Genesis and evolution of the 1997–98 El Niño. *Science*, **283**, 950–954, <https://doi.org/10.1126/science.283.5404.950>.

NHC, 2024: 2023 North Atlantic hurricane tracking chart (preliminary). NOAA, accessed 21 March 2024, https://www.nhc.noaa.gov/tafb_latest/tws_atl_latest.gif.

Peng, P., A. Kumar, M. S. Halpert, and A. G. Barnston, 2012: An analysis of CPC’s operational 0.5-month lead seasonal outlooks. *Wea. Forecasting*, **27**, 898–917, <https://doi.org/10.1175/WAF-D-11-00143.1>.

—, —, M. Chen, Z.-Z. Hu, and B. Jha, 2019: Was the North American extreme climate in winter 2013/14 a SST forced response? *Climate Dyn.*, **52**, 3099–3110, <https://doi.org/10.1007/s00382-018-4314-0>.

Shi, J., A. V. Fedorov, and S. Hu, 2019: North Pacific temperature and precipitation response to El Niño-like equatorial heating: Sensitivity to forcing location. *Climate Dyn.*, **53**, 2731–2741, <https://doi.org/10.1007/s00382-019-04655-x>.

Swenson, E. T., D. M. Straus, C. E. Snide, and A. al Fahad, 2019: The role of tropical heating and internal variability in the California response to the 2015/16 ENSO event. *J. Atmos. Sci.*, **76**, 3115–3128, <https://doi.org/10.1175/JAS-D-19-0064.1>.

Wang, H., and Coauthors, 2014: How well do global climate models simulate the variability of Atlantic tropical cyclones associated with ENSO? *J. Climate*, **27**, 5673–5692, <https://doi.org/10.1175/JCLI-D-13-00625.1>.